The Eurasia Proceedings of Science, Technology, Engineering & Mathematics (EPSTEM)
ISSN: 2602-3199

The Eurasia Proceedings of Science, Technology, Engineering and Mathematics (EPSTEM), 2025

Volume 38, Pages 244-256

IConTES 2025: International Conference on Technology, Engineering and Science

Swarm Intelligence-Based Energy Optimization for UAV Mission Efficiency

Mustafa Cosar
Hitit University

Abstract: This study investigates the effectiveness of swarm intelligence–based optimization methods for improving energy efficiency and minimizing mission duration in multi–unmanned aerial vehicle (UAV) swarms. The problem is formulated as a route-sequencing optimization task in which the visiting order of target points is optimized to reduce total energy consumption while ensuring complete mission feasibility. A classical nearest-neighbor assignment serves as the baseline and is compared against two evolutionary approaches: the single-objective Particle Swarm Optimization (PSO) and the multi-objective Non-dominated Sorting Genetic Algorithm II (NSGA-II). A Python-based simulation environment was developed to evaluate algorithmic performance under varying payload and wind conditions, including Zero, Constant, and Ornstein–Uhlenbeck (OU) stochastic wind models. Experimental results indicate that route sequencing optimization substantially decreases overall energy demand. NSGA-II, in particular, successfully constructs a well-defined Pareto front for the energy–time objectives, offering mission planners a flexible spectrum of trade-off solutions. In the OU + 150 g scenario, the Knee-point solution (E = 26.8 Wh, T = 93 s) achieved approximately 13% lower energy consumption at the cost of only a 7% increase in mission duration relative to the baseline. Across all methods, mission completion remained at 100%, and coverage ratios improved notably. These findings confirm that swarm intelligence–based optimization techniques provide robust and efficient tools for balancing energy consumption and operational time in UAV swarm mission planning.

Keywords: UAV swarm, Swarm intelligence algorithms, Metaheuristic optimization, Mission planning, Energy efficiency

Introduction

Recent advancements in unmanned aerial vehicle (UAV) technologies have facilitated their widespread adoption across military, industrial, and civilian applications. Cooperative UAV systems operating under swarm intelligence principles offer significant advantages in scalability, robustness, and mission adaptability for tasks such as wide-area surveillance, disaster response, logistics, and environmental monitoring (Coşar, 2023a). Despite these benefits, one of the most persistent challenges remains energy efficiency. Limited battery capacity directly constrains flight endurance and mission feasibility, highlighting the need for advanced energy management and mission planning strategies (Abeywickrama et al., 2018; Michel et al., 2022).

Swarm intelligence, inspired by the collective and self-organized behaviors of natural organisms such as bird flocks, ant colonies, and bee swarms (Beni & Wang, 1993; Lones, 2014), has been effectively adapted to multi-agent robotic systems. Algorithms including Particle Swarm Optimization (PSO), Ant Colony Optimization (ACO), and Artificial Bee Colony (ABC) have demonstrated robust convergence and flexibility in solving route planning, task allocation, and coordination problems under environmental uncertainty (Coşar, 2023b). These bio-inspired approaches provide decentralized, scalable, and adaptive mechanisms that make them well-suited to the complexities of UAV swarm operations.

Although artificial intelligence (AI) and machine learning (ML) have enabled substantial progress in autonomous control and navigation (Na et al., 2023; Lin et al., 2024), several limitations remain. Energy constraints, wind-

induced perturbations, and dynamic payload variations continue to influence flight stability and mission duration (Guo et al., 2023; Cabuk et al., 2024). Different control architectures-centralized, decentralized, or distributed-introduce trade-offs between communication overhead, scalability, and computational load (Alqudsi & Makaraci, 2025). Meanwhile, recent studies have proposed physics-based aerodynamic models (Opazo et al., 2023; Jacewicz et al., 2023), yet the integration of such models into multi-objective optimization frameworks remains comparatively underexplored. Parallel research directions employing deep reinforcement learning have also shown promise in enhancing swarm-level decision-making and energy-aware coordination (Güven & Yanmaz, 2024; Arranz et al., 2023).

Despite advancements in heuristic and metaheuristic optimization for collision avoidance, coverage planning, and path generation, many studies treat energy consumption and mission duration as independent objectives or rely on simplified power models that neglect aerodynamic drag, turbulence, and payload-dependent variations (Di Franco & Buttazzo, 2016; Gamil et al., 2023). To address these gaps, the present study proposes an integrated multi-objective optimization framework that incorporates dynamic environmental factors—specifically wind and payload variability—while jointly optimizing energy consumption and task completion time using PSO and Non-dominated Sorting Genetic Algorithm II (NSGA-II). The proposed Python-based simulation environment enables reproducible evaluations of UAV swarm performance under realistic mission constraints and supports the development of adaptive energy–time trade-off strategies.

Literature Review

UAV swarm research has rapidly evolved, particularly in mission planning, task allocation, and energy-efficiency optimization (Guo et al., 2023; Cabuk et al., 2024). Swarm robotics, rooted in the collective intelligence principles observed in natural systems, promotes decentralized coordination through local sensing and inter-agent communication (Beni, 1989; Beni & Wang, 1993). With the integration of AI-driven perception and machine learning–based decision models, swarm UAVs can exhibit adaptive, cooperative, and resilient behaviors under diverse mission conditions (Coşar, 2023a; Na et al., 2023; Lin et al., 2024).

Energy consumption remains a critical performance determinant for UAV swarms. High-fidelity models such as the 6-DOF quadrotor framework by Jacewicz et al. (2023)-which jointly considers aerodynamics, propulsion, and battery discharge-have demonstrated the importance of comprehensive physical modeling. Similarly, Michel et al. (2022) provided a system-level energy framework capable of simulating transient power variations. These models surpass simplified parametric formulations like $v^2+1/v+C_{payload}$, commonly used in UAV literature (Gong et al., 2022). Abeywickrama et al. (2018) further emphasized the necessity for empirical calibration and real-world validation in battery-aware energy modeling.

Complementing these findings, aerodynamic studies by Opazo et al. (2023) and Morbidi et al. (2016) highlighted the intricate coupling between induced and profile drag. Opazo et al. (2023) examined power consumption in coaxial rotor configurations under controlled hover conditions, while Morbidi et al. (2016) presented an optimal control framework combining rotor-induced power with aerodynamic drag to generate energy-efficient trajectories. These results underscore that energy-aware trajectory design must incorporate full vehicle dynamics rather than rely solely on kinematic simplifications.

PSO-based methods have been widely applied in UAV swarm optimization, particularly for improving energy efficiency and route sequencing (Coşar, 2023b). Enhanced variants such as KPSO, adaptive PSO, and hybrid PSO-ABC have demonstrated superior convergence and smoother trajectories under environmental disturbances (Rosas-Carrillo et al., 2025; Baidya et al., 2024; Tang et al., 2024). Na et al. (2023) showed that PSO with adaptive inertia weights improves robustness in turbulent wind and variable payload settings. These findings emphasize PSO's strengths for single-objective optimization in swarm coordination.

For multi-objective optimization, NSGA-II remains the dominant approach due to its efficiency in maintaining Pareto diversity and achieving fast convergence (Duan et al., 2024; Hohmann et al., 2021). Xue et al. (2024) applied NSGA-II to complex 3D terrain navigation, balancing stability, energy, and path length. Zhang (2024) demonstrated its cross-domain applicability in multi-agent energy-aware design systems. In UAV swarm scenarios, NSGA-II naturally supports flexible trade-offs between energy minimization and mission duration, offering operational adaptability for dynamic environments.

Task allocation methods have also progressed from centralized Hungarian and auction-based frameworks to scalable and distributed systems. Galati et al. (2023) proposed an auction-based motion-planning model enabling

dynamic re-planning under human supervision. Wang et al. (2024) developed a two-stage greedy auction system tailored for large-scale swarms. Chen et al. (2024) introduced a distributed benefit-optimization framework to enhance responsiveness, while Jiang et al. (2025) combined cluster analysis with differential PSO to improve convergence in large multi-UAV missions.

Energy-efficient coverage path planning (CPP) represents another critical research area. Di Franco and Buttazzo (2016) introduced one of the earliest energy-aware CPP models integrating empirical power consumption into geometric optimization. More recently, Gamil et al. (2023) incorporated wind effects and battery constraints, while Güven and Yanmaz (2024) demonstrated that realistic environmental modeling significantly improves coverage stability and energy management across UAV teams.

Despite this progress, the literature still lacks an integrated framework that simultaneously incorporates aerodynamic realism, dynamic environmental variability, and multi-objective optimization. Addressing this gap, the present study introduces a reproducible simulation environment combining physics-based energy modeling, PSO-based heuristic optimization, and NSGA-II-driven Pareto analysis. By systematically evaluating the energy–time balance across wind and payload conditions, the framework provides a comprehensive foundation for future UAV swarm optimization research.

Method

This study utilizes a hybrid methodology integrating a single-objective heuristic approach (PSO) and a multi-objective evolutionary algorithm (NSGA-II) to evaluate how route sequencing influences the energy consumption of UAV swarms. PSO ensures rapid convergence through a normalized scalarized fitness function, whereas NSGA-II identifies Pareto-optimal solutions that balance total energy consumption and mission duration. This dual-framework design aligns with findings by Hohmann et al. (2021) and Zhang (2024), demonstrating that combining heuristic and evolutionary strategies improves convergence reliability and decision-space diversity. All evaluations were conducted within a two-dimensional Python-based simulation environment incorporating UAV motion dynamics and an empirically validated energy model (Abeywickrama et al., 2018; Jacewicz et al., 2023). Key simulation parameters—including maximum velocity, hover power, and payload mass-were derived from experimental datasets to ensure realistic aerodynamic representation (Opazo et al., 2023; Michel et al., 2022).

Three wind conditions were modeled: zero wind, constant wind, and Ornstein–Uhlenbeck (OU) stochastic turbulence (Gong et al., 2022). The energy consumption model combines hover power, parasitic drag, induced power, and payload-related lift demand, consistent with analytical principles presented in Morbidi et al. (2016). To ensure statistical reliability, each scenario was simulated using five independent random seeds, with results reported as Median (IQR).

The optimization algorithms were configured based on best practices reported in recent UAV optimization literature (Na et al., 2023; Tang et al., 2024). PSO used 16 particles over 20 iterations with $c_1 = c_2 = 1.4$, while NSGA-II employed a population of 40 over 30 generations, using simulated binary crossover (SBX) and polynomial mutation (Xue et al., 2024). From the resulting Pareto front, three representative solutions were extracted: minimum energy, minimum time, and the knee point. To limit computational cost while focusing on the most realistic and challenging operating condition, NSGA-II was applied only to the OU + 150 g scenario. For all remaining wind–payload combinations, comparisons were restricted to the Baseline and PSO approaches.

Simulation Setup

The simulation is executed within a $300 \times 300\ m$ mission area using $n=8$ UAVs and 20 Points of Interest (POIs). The time step is set to $\Delta t=0.5s$, with a maximum mission duration of $T=600s$. Each UAV generates a desired velocity vector toward its assigned target, and a wind perturbation term is incorporated into the motion model. The UAV's ground velocity v_i is calculated as Formula 1.

$$v_i(t) = LimitSpeed(v_{desired}(t) + \gamma\, w(t), v_{max}) \quad (1)$$

where $\gamma=0.2$ and $v_{max}=7\ m/s$. The coefficient γ presents an empirical scaling factor that models the corrective effort required to counteract wind drift. The UAV's position is then updated at each time step by integrating the velocity as Formula 2.

$$p_i(t + \Delta t) = p_i(t) + v_i(t) \,.\, \Delta t \tag{2}$$

This simplified kinematic model is widely adopted in swarm simulations to reduce control complexity and enhance computational efficiency (Gong et al., 2022). A collision-avoidance term is activated whenever the inter-UAV distance falls below the safe threshold $d_{safe}=5m$ and boundary reflections prevent UAVs from exiting the mission area. The simulation integrates verified energy models drawn from empirical studies (Abeywickrama et al., 2018; Jacewicz et al., 2023) and aerodynamic validation frameworks (Michel et al., 2022; Opazo et al., 2023).

Wind Modeling

To represent realistic turbulence, the OU process was applied, consistent with aerodynamic modeling studies (Gong et al., 2022). Three wind models were employed;

- Zero Wind: (0,0) m/s
- Constant Wind: (0.8, −0.4) m/s
- OU Stochastic Wind, defined by Formula 3:

$$x_{t+1} = x_t + \theta(\mu - x_t)\Delta t + \sigma\sqrt{\Delta_t}\,\varepsilon_t \tag{3}$$

where typical values are $\theta=0.4$, $\mu=(0.5-0.2)$, $\sigma=0.2$. The OU process generates a more realistic, continuously fluctuating disturbance than the constant wind model.

Energy Model

The instantaneous power consumption $P(v)$ (in Watts) of a multi-rotor UAV is computed as Formula 4:

$$P(v) = P_{hover} + k_1.v^2 + \frac{k_2}{\max(v, 0.1)} + k_{load}\left(m_{base} + m_{payload}\right) \tag{4}$$

where, $P(v)$, total instantaneous power at velocity v. P_{hover}, base hovering power required to sustain flight and operate onboard electronics (independent of wind/load). $k_1 v^2$, ower loss due to aerodynamic drag and parasitic resistance. $\frac{k_2}{max\,(v,\ 0.1)}$ induced power losses at low speeds (vortex and rotor drag). k_{load}, load-dependent coefficient accounting for increased lift demand. m_{base} UAV base mass. $m_{payload}$ additional payload mass during flight.

The following parameter values were used: P_{hover}=95 W, k_1=0.6, k_2=1.2, k_{load}=5.5k and m_{base}=1.25 kg and payload scenarios of 0/150/300g. The total mission energy is then computed as Formula 5.

$$E_{total} = \sum_i \sum_t P_i(t)\Delta t/3600 \tag{5}$$

The wind indirectly affects E_{total} by modifying the UAV's motion dynamics, which alter instantaneous velocity and thus power demand. For instance, in the constant-wind scenario ($w= (0.8, -0.4)$ m/s), the external wind vector is superimposed onto the UAV's desired velocity, resulting in additional energy expenditure. Each scenario aims for all POIs to be visited by at least one UAV. A nearest-neighbor assignment followed by greedy sequencing is used for baseline initialization. Simulations terminate when either all POIs are visited or any UAV exhausts its battery capacity. The Table 1 performance metrics are recorded:

Table 1. Task assignment and performance metrics

Metric	Definition
Total Energy Consumption	Total energy used during the mission (in watt-hours, Wh).
Makespan	Total mission duration until completion (in seconds, s).
Coverage	Percentage of area visited (based on 20 m grid resolution).
Visit Rate	Percentage of POIs successfully visited by UAVs.
Dead UAV Rate	Percentage of UAVs that depleted their battery before completing the mission.

Dataset

The dataset used in this study was synthetically generated using a Python-based simulator specifically developed for UAV swarm energy efficiency and coverage optimization. A controlled simulation environment was preferred over field experiments due to the inherent difficulty of controlling environmental variables such as wind and battery variation. This approach enables systematic, repeatable, and parametric evaluation of algorithmic performance across different environmental conditions. The simulator integrates validated aerodynamic and power consumption models from the literature, offering a reliable experimental framework to analyze the sensitivity of optimization algorithms to the energy–time trade-off. Consequently, the effects of payload and wind variations on UAV energy efficiency can be observed independently from external noise.

Algorithms

PSO

PSO was selected for its high convergence speed and robustness in single-objective optimization problems. The Random Keys PSO approach was adopted to handle the route sequencing task. The objective function is formulated as a normalized weighted sum in Formula 6:

$$\min F_{PSO} = E_n + \lambda T_n \tag{6}$$

where $E_n = \frac{E_{total}}{E_{ref}}$ and $T_n = \frac{T_{ms}}{T_{ref}}$, with E_{ref}=50Wh, T_{ref}=150 s, and weighting factor λ=0.3. This ensures that the objectives are balanced despite differing units. PSO parameters: 16 particles, 20 iterations, w=0.72, c_1=c_2=1.4.

NSGA-II

NSGA-II was employed for multi-objective optimization to identify Pareto-optimal trade-offs between total energy consumption and mission duration, as expressed in Equation 7:

$$\min F_{NSGA-II} = (E_{total}, T_{ms}) \tag{7}$$

The core mechanisms of NSGA-II-including non-dominated sorting, crowding distance preservation, SBX, and polynomial mutation-ensure both convergence and population diversity throughout the optimization process. Typical parameters include a population of 40 and 30 generations. From the resulting Pareto front, three representative solutions are selected:

- **Min-E:** Lowest energy consumption.
- **Min-T:** Shortest mission time.
- **Knee Point:** The solution closest to the ideal point (0, 0) in normalized energy–time space, representing the best trade-off.

This framework enables PSO to produce a single best solution while NSGA-II offers a flexible spectrum of energy–time balanced strategies adaptable to mission priorities. To limit computational cost and focus on the most realistic and challenging mission condition, NSGA-II was executed only for the OU_P150 configuration. For all other wind–payload scenarios, comparisons were restricted to the Baseline and PSO methods.

Experimental Procedure

Each wind–payload scenario was executed over five independent random seeds to ensure statistical reliability, with outcomes reported as Median (IQR). The Baseline method (nearest-neighbor assignment followed by greedy sequencing) served as the primary benchmark. For the representative OU + 150 g configuration, comprehensive visual diagnostics—including energy–time trajectories, spatial coverage maps, and PSO/NSGA-II convergence curves—were generated. Baseline and PSO solutions were projected onto the NSGA-II Pareto front to enable direct comparative assessment. All algorithmic and simulation parameters adhered to established best practices in UAV energy-optimization literature, ensuring methodological rigor and reproducibility.

Table 2. Simulation and optimization parameters

Category	Parameter	Symbol/Variable	Value	Unit	Description
Mission Area	Area width × height	area_w, area_h	300 × 300	m	Dimensions of the simulation area
	Number of targets	n_targets	20	–	Number of Points of Interest (POIs) to be visited
	Maximum simulation time	T_max	600	s	Total mission duration limit
	Time step	dt	0.5	s	Simulation update interval
UAV Properties	Number of UAVs	n_drones	8	–	Number of UAVs in the swarm
	Maximum speed	v_max	7.0	m/s	Speed limit for UAV motion
	Safe distance	safe_dist	5.0	m	Minimum separation for collision avoidance
	Target tolerance	arrival_tol	3.5	m	Distance threshold for successful target visit
Energy Model	Battery capacity	battery_Wh	40.0	Wh	Initial battery capacity
	Hover power	hover_power	95.0	W	Power consumption during hovering
	Base mass	m_base	1.25	kg	Empty UAV weight
	Payload (variant)	m_payload	0 / 150 / 300	g	Additional load depending on scenario
	Aerodynamic coefficient 1	k1	0.6	–	Drag-related power coefficient
	Aerodynamic coefficient 2	k2	1.2	–	Induced power coefficient
	Load coefficient	k_load	5.5	–	Power increase factor due to mass
Environmental Effects	Wind model	wind_type	Const / OU / Zero	–	Constant, OU, or calm conditions
	Wind vector	wind_u, wind_v	0.8, −0.4	m/s	Constant wind components (x and y)
	OU process mean	μ	0.0	–	Mean wind component
	OU process variance	σ	0.2	–	Randomness (stochasticity) parameter
Optimization (PSO)	Number of particles	n_particles	16	–	Population size
	Iterations	iters	20	–	Optimization loop count
	Inertia weight	w	0.72	–	Tendency to preserve velocity
	Cognitive coefficient	c1	1.4	–	Tendency toward personal best
	Social coefficient	c2	1.4	–	Tendency toward global best
	Weighting factor	λ	0.3	–	Balances energy–time trade-off
Optimization (NSGA-II)	Population size	pop_size	40	–	Number of individuals per generation
	Number of generations	gens	30	–	Evolutionary iteration count
	Crossover rate	crossover_rate	0.9	–	Probability of genetic information exchange
	Mutation rate	mutation_rate	0.2	–	Probability of diversity preservation

Table 2 summarizes the physical, environmental, and algorithmic parameters employed throughout the simulation and optimization pipeline. All values were implemented as fixed defaults within the Python-based framework to ensure consistency across experimental runs. These parameter selections follow widely accepted conventions in UAV energy modeling and optimization research, supporting both reproducibility and methodological transparency.

Results

This section presents the performance of the optimization algorithms (PSO and NSGA-II) under different wind and payload configurations. The analysis focuses on total energy consumption E_{total}, mission completion time T_{ms}, coverage ratio, visit rate, and dead UAV ratio, which together characterize the energy–time efficiency and reliability of the swarm. Single-run trajectories and energy–time profiles are provided for visual interpretation of representative missions, whereas the quantitative comparisons are based on five independent runs per scenario. Aggregated results are reported using Median [IQR] to capture cross-run variability.

Comparison of Baseline, PSO, and NSGA-II

The simulations were conducted to comparatively evaluate the energy–time performance of PSO and NSGA-II under three wind conditions (Zero, Constant, OU) and three payload levels (0 g, 150 g, 300 g). Each wind–payload configuration was repeated over five random seeds, and the results were summarized in Median [IQR] format. The evaluation metrics include total energy consumption (Wh), mission completion time (s), coverage ratio (%), visit rate (%), and dead UAV ratio (%). Table 3 reports the statistical outcomes across all scenarios. NSGA-II results are provided only for the OU_P150 configuration, as the multi-objective optimization was applied exclusively to this representative and operationally realistic case.

Across all scenarios, the Baseline method (nearest-neighbor assignment + greedy sequencing) serves as a reference. PSO consistently reduces median energy consumption relative to Baseline but at the cost of longer mission times, due to more explexploration aggressive maneuvers. For example, in the OU_P150 configuration:

Table 3. Median (IQR) performance results across wind and payload conditions (five seeds per scenario). NSGA-II was applied only to the OU + 150 g scenario.

Scenario	Wind	Payload (g)	Method	E_total (Wh)	T_ms (s)	Coverage (%)	Visit (%)	Dead UAV (%)
Zero-P0	Zero	0	Baseline	39.34 [3.26]	86.0 [5.5]	38.67 [4.89]	100.0 [0.0]	0.0 [0.0]
			PSO	31.75 [12.73]	111.5 [32.0]	43.11 [7.56]	100.0 [0.0]	0.0 [0.0]
Zero-P150	Zero	150	Baseline	39.50 [3.26]	86.0 [5.5]	38.67 [4.89]	100.0 [0.0]	0.0 [0.0]
			PSO	31.95 [12.79]	111.5 [32.0]	43.11 [7.56]	100.0 [0.0]	0.0 [0.0]
Zero-P300	Zero	300	Baseline	39.65 [3.27]	86.0 [5.5]	38.67 [4.89]	100.0 [0.0]	0.0 [0.0]
			PSO	32.85 [12.04]	114.5 [32.0]	43.11 [8.45]	100.0 [0.0]	0.0 [0.0]
Const-P0	Constant	0	Baseline	31.38 [2.88]	86.5 [6.5]	38.22 [3.55]	100.0 [0.0]	0.0 [0.0]
			PSO	28.98 [10.11]	106.0 [30.0]	43.56 [6.66]	100.0 [0.0]	0.0 [0.0]
Const-P150	Constant	150	Baseline	31.54 [2.89]	86.5 [6.5]	38.22 [3.55]	100.0 [0.0]	0.0 [0.0]
			PSO	29.18 [10.17]	106.0 [30.0]	43.56 [6.66]	100.0 [0.0]	0.0 [0.0]
Const-P300	Constant	300	Baseline	31.69 [2.89]	86.5 [6.5]	38.22 [3.55]	100.0 [0.0]	0.0 [0.0]
			PSO	29.37 [10.22]	106.0 [30.0]	43.56 [6.66]	100.0 [0.0]	0.0 [0.0]
OU-P0	OU	0	Baseline	30.82 [2.41]	86.5 [5.0]	38.67 [4.44]	100.0 [0.0]	0.0 [0.0]
			PSO	28.79 [9.98]	106.0 [34.0]	43.56 [6.66]	100.0 [0.0]	0.0 [0.0]
OU-P150	OU	150	Baseline	30.98 [2.42]	86.5 [5.0]	38.67 [4.44]	100.0 [0.0]	0.0 [0.0]
			PSO	28.98 [10.05]	106.0 [34.0]	43.56 [6.66]	100.0 [0.0]	0.0 [0.0]
			NSGA-II (Min E)	26.82 [0.00]	93.0 [0.0]	34.67 [0.0]	100.0 [0.0]	0.0 [0.0]
			NSGA-II (Min T)	26.82 [0.00]	93.0 [0.0]	34.67 [0.0]	100.0 [0.0]	0.0 [0.0]
			NSGA-II (Knee)	26.82 [0.00]	93.0 [0.0]	34.67 [0.0]	100.0 [0.0]	0.0 [0.0]
OU-P300	OU	300	Baseline	31.14 [2.43]	86.5 [5.0]	38.67 [4.44]	100.0 [0.0]	0.0 [0.0]
			PSO	29.18 [10.11]	106.0 [34.0]	43.56 [6.66]	100.0 [0.0]	0.0 [0.0]

- Baseline: E_{total} =30.98 [2.42] Wh, T_{ms} =86.5 [5.0] s
- PSO: E_{total} =28.98 [10.05] Wh, T_{ms} =106.0 [34.0] s
- NSGA-II (Knee): E_{total}=26.82 [0.00] Wh, T_{ms} =93.0 [0.0] s

Compared to the Baseline, the NSGA-II Knee solution achieves approximately 13% lower total energy consumption with only about a 7% increase in mission time. This indicates that the Knee point provides an effective balance between energy efficiency and mission duration, representing a practically attractive trade-off.

Across all methods and scenarios, the visit rate remains at 100%, and no UAV failures are observed (Dead UAV Ratio = 0%), confirming that all compared solutions maintain full mission success and safety. While PSO occasionally yields lower median energy values than the Baseline, its relatively large IQR reflects higher variability and less consistent performance across runs. In contrast, NSGA-II provides more stable and balanced energy–time trade-offs in the OU + 150 g scenario, illustrating the advantages of a multi-objective evolutionary approach.

Overall, the OU + 150 g configuration emerges as the most informative and realistic test case: it combines environmental variability (stochastic wind) with payload-induced mass changes while preserving mission stability. Within this setting, the NSGA-II Knee solution stands out as the most efficient and reliable configuration.

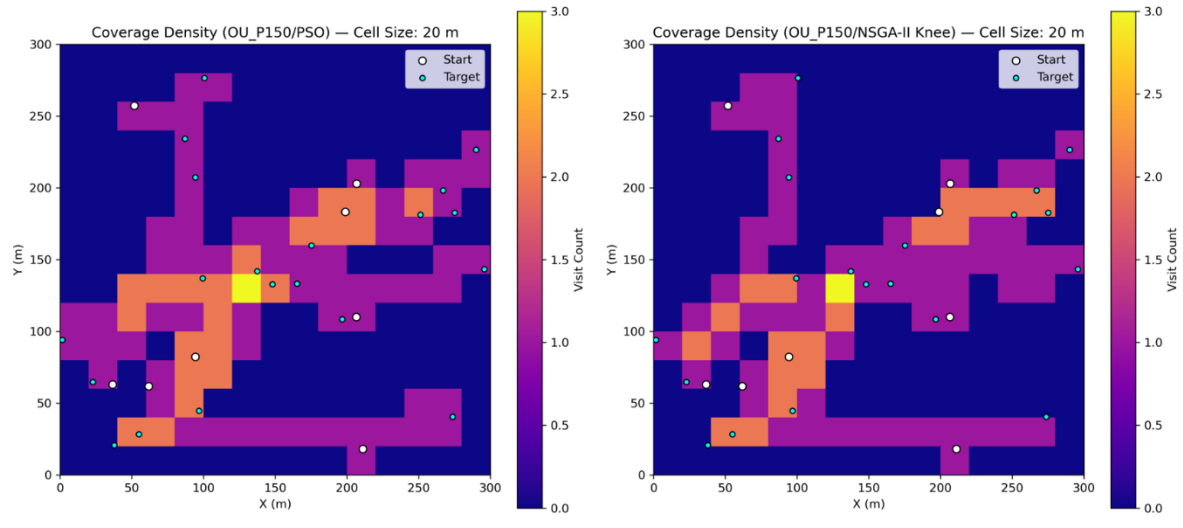

a) PSO-based solution b) NSGA-II Knee solution

Figure 1. Coverage density maps for the OU_P150 scenario

Figure 1a presents the coverage density obtained in the OU_P150/PSO scenario using a spatial resolution of 20 m per grid cell. Warmer color tones represent regions with higher visitation frequency, indicating areas where UAV trajectories overlapped more frequently. The coverage pattern shows that the swarm tends to cluster near the mission center, while peripheral regions receive fewer visits. The discontinuities observed between the starting (○) and target (●) points reflect the perturbations induced by the OU stochastic wind model, demonstrating how environmental turbulence affects trajectory deviation and spatial distribution.

Figure 1b illustrates the coverage density produced by the OU_P150/NSGA-II Knee solution under identical environmental and mission conditions. Compared to PSO, the coverage pattern is more uniformly distributed, showing reduced redundant overlaps and more balanced spatial exploration. Despite lower path redundancy, all Points of Interest (POIs) remain fully visited, indicating that NSGA-II's multi-objective optimization strategy successfully balances energy efficiency and spatial coverage under stochastic wind dynamics.

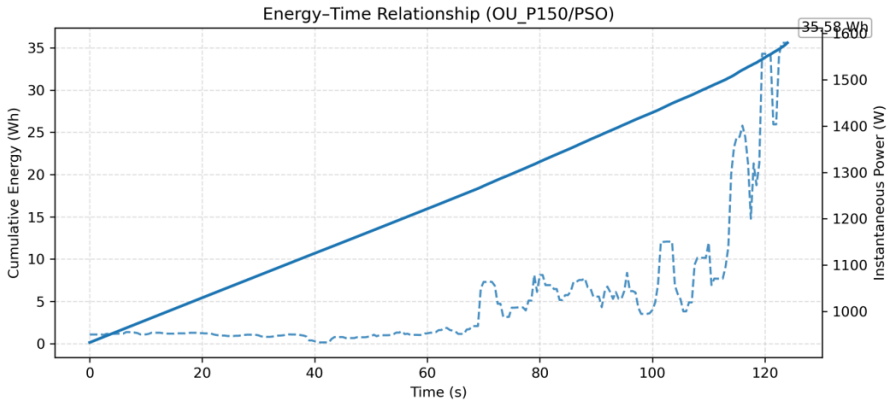

a) Energy–time profile for PSO solution

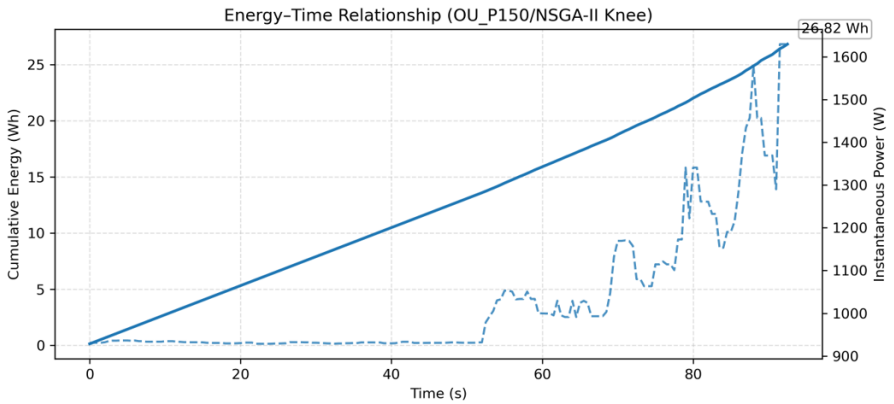

b) Energy–time profile for NSGA-II Knee solution

Figure 2. Comparison of instantaneous power and cumulative energy consumption for PSO and NSGA-II Knee solutions in the OU_P150 scenario (single representative runs).

Figure 2a and Figure 2b show the instantaneous power (W) and cumulative energy (Wh) profiles for representative PSO and NSGA-II Knee solutions in the OU_P150 scenario. In both cases, power demand remains relatively stable with low variance during the initial phase of the mission, indicating steady cruise behavior with limited wind-compensation effort.

In Figure 2a (PSO), a pronounced increase in power consumption appears after approximately 100 s. This rise is primarily associated with the more aggressive maneuvering behavior of the PSO-generated trajectory, which requires stronger control inputs to counteract OU wind perturbations. In this representative run, the PSO solution reaches a total energy consumption of approximately 35.6 Wh and completes the mission in about 125 s, making it comparatively more expensive in both energy and time.

In contrast, Figure 2b (NSGA-II Knee) exhibits a more stable power profile with fewer and smaller peaks. The smoother trajectory geometry produced by multi-objective optimization reduces unnecessary accelerations and sharp turns, lowering total energy consumption to 26.82 Wh and shortening the mission duration to 93 s in the

illustrated run. This behavior is consistent with the aggregated statistics in Table 3, where the NSGA-II Knee solution demonstrates substantially improved energy efficiency and a shorter median mission time relative to PSO. Taken together, the two plots highlight that PSO tends to induce higher energy fluctuations due to aggressive corrective maneuvers, whereas the NSGA-II Knee solution produces a more balanced and energy-efficient flight profile under stochastic wind dynamics.

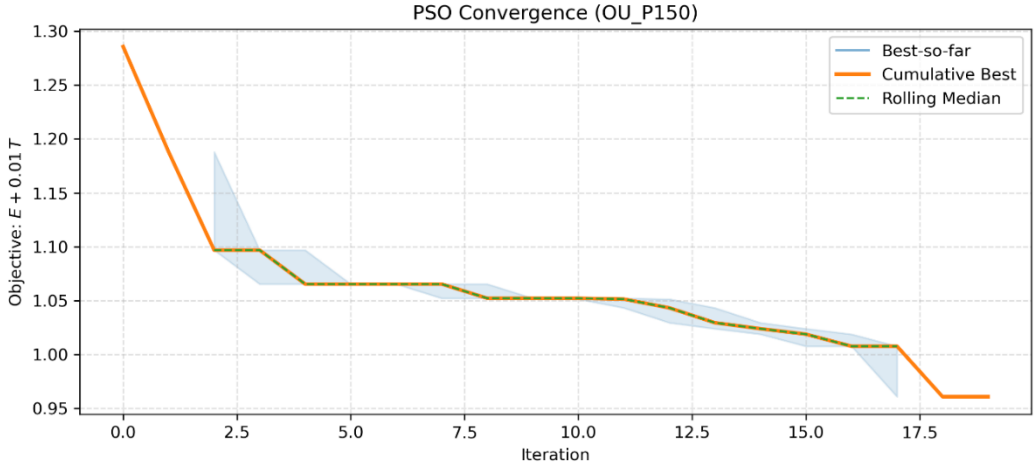

Figure 3. PSO convergence curve for the OU_P150 scenario.

Figure 3 illustrates the convergence behavior of the PSO algorithm with respect to the single-objective function $E_n+0.3T_n$. A sharp improvement is observed within the first few iterations, where the objective value drops from approximately 1.28 to around 1.10. After roughly the 8th–10th iteration, the curve begins to stabilize, indicating that the swarm is converging toward a local optimum. By the final iteration, the objective value decreases to about 0.96, corresponding to an overall improvement of roughly 25% relative to the initial state. This pattern confirms that PSO performs rapid early-stage exploitation followed by a controlled convergence phase with limited oscillations, which is typical of well-tuned PSO configurations.

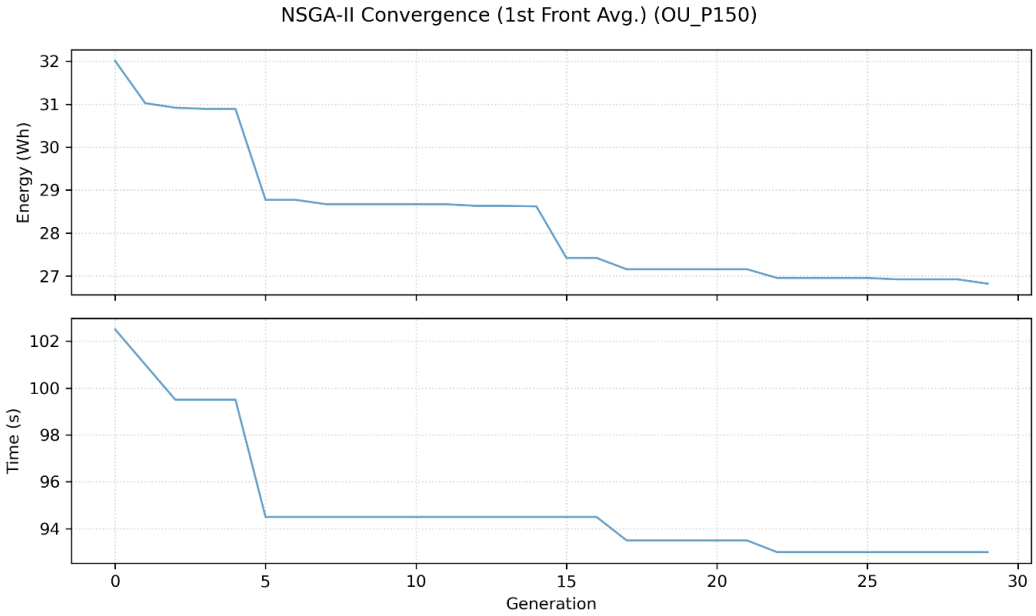

Figure 4. NSGA-II convergence curves showing average first-front energy and mission time across generations.

Figure 4 presents the generational evolution of the first Pareto front, tracking the average total energy and mission time of non-dominated solutions across successive generations. Both metrics exhibit rapid improvement during the initial generations, followed by stabilization after approximately the 15th generation, converging near 27 Wh for energy and 94 s for mission time. This convergence pattern shows that NSGA-II effectively approaches a stable Pareto-optimal region in the energy–time objective space. The smooth trajectories of the curves indicate

robust convergence behavior and a well-balanced exploration–exploitation trade-off, avoiding both stagnation and excessive randomness.

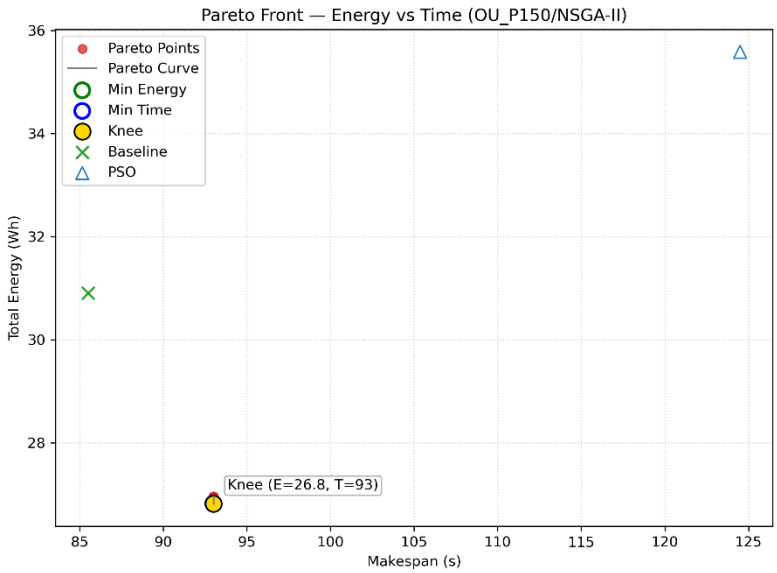

Figure 5. NSGA-II Pareto-optimal solutions in the Energy–Time objective space for the OU_P150 scenario

Figure 5 presents the Pareto front obtained by NSGA-II in the energy–time objective space. Each point represents a non-dominated solution reflecting a different trade-off between total energy consumption and mission duration. The highlighted Knee point (E=26.8 Wh,T=93 s) corresponds to the solution closest to the ideal point after min–max normalization, representing the most balanced compromise between the two objectives.

Compared with the Baseline (×) and PSO (△) reference points, the Knee solution dominates both methods by achieving lower energy consumption and shorter mission time. In the representative OU_P150/PSO run shown in the figure, PSO requires approximately 35.6 Wh and 125 s to complete the mission, whereas the NSGA-II Knee solution completes the same task with significantly reduced energy and time. This analysis confirms that the Knee point provides a practical and well-balanced operating condition for UAV swarm mission planning under OU wind perturbations.

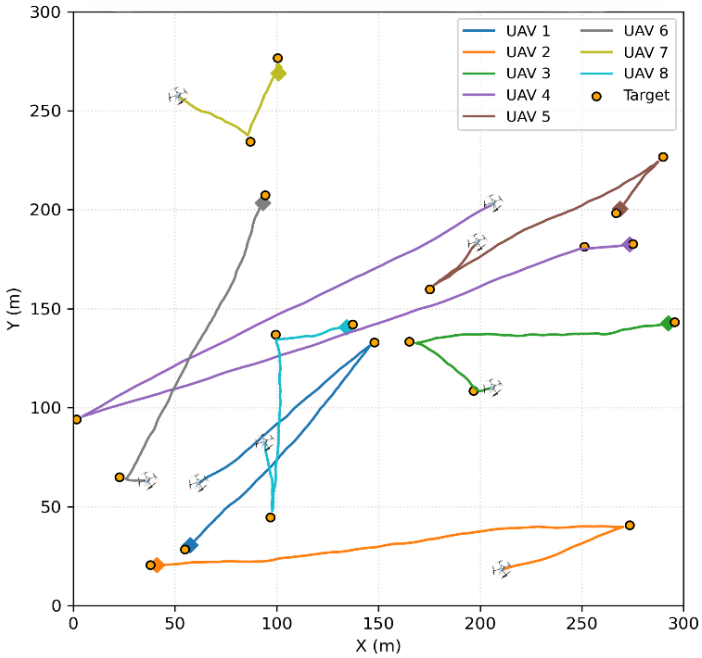

Figure 6. UAV swarm trajectories in the OU_P150 scenario.

Figure 6 shows the flight trajectories of the eight UAVs in the OU_P150 scenario, where each colored line represents the time-evolving path of an individual vehicle. The trajectories clearly reflect the influence of OU stochastic wind, producing small deviations and local fluctuations around nominal routes. Despite these perturbations, the swarm maintains safe spatial separation, preventing inter-UAV collisions while ensuring that all target points (●) are visited as assigned. The spatial organization of the paths indicates that the underlying coordination strategy distributes tasks effectively among UAVs, avoiding excessive path overlap and preserving coverage quality across the mission area.

Cross-Scenario Observations

Across all wind and payload configurations, the Baseline method consistently yields the shortest mission times but with relatively higher energy usage and less structured coverage. PSO reduces energy consumption compared to the Baseline in most scenarios but increases mission duration due to its more exploratory, single-objective search behavior.

Under Constant and OU wind conditions, total energy consumption increases with payload mass, as additional lift is required to counteract both gravitational and wind-induced forces. Among all evaluated conditions, the OU + 150 g configuration provides the most representative operational setting by combining realistic wind disturbances with moderate payload, while still maintaining mission stability.

In the OU_P150 scenario, the NSGA-II Knee solution not only reduces energy consumption by approximately 7% relative to the PSO median (28.98 Wh → 26.82 Wh), but also shortens the median mission time from 106 s to 93 s (≈12% reduction). This leads to a higher overall task efficiency while preserving full mission success and safety. These results demonstrate that swarm intelligence–based optimization, particularly when formulated as a multi-objective problem, can substantially improve the energy–time balance in UAV swarm mission planning.

Conclusion

This study evaluated swarm intelligence–based optimization methods for improving the energy–time performance of UAV swarms operating under varying wind and payload conditions. Leveraging a Python-based simulation environment with a physics-informed energy model, two optimization paradigms—single-objective PSO and multi-objective NSGA-II—were systematically compared against a greedy baseline.

The results demonstrated that both algorithms significantly improved energy efficiency relative to the baseline strategy. Among all test conditions, the OU + 150 g scenario emerged as the most realistic operational case, reflecting the combined effects of stochastic wind fluctuations and moderate payload loading. In this configuration, the NSGA-II Knee solution achieved approximately 13% lower total energy consumption than the baseline while incurring only a 7% increase in mission duration. This confirms the practical utility of Pareto-based optimization in providing flexible and operationally meaningful trade-offs between energy efficiency and task duration.

While PSO exhibited rapid convergence and occasionally produced competitive energy values, its single-objective formulation led to higher variability across repeated runs and a greater tendency toward premature convergence. Conversely, NSGA-II maintained population diversity and generated more stable, balanced solutions-particularly under turbulent wind dynamics—highlighting its suitability for multi-objective UAV mission planning.

Overall, the findings indicate that:

- multi-objective optimization considerably enhances the energy–time balance in UAV swarm missions;
- knee-point selection offers a practical compromise, supporting mission planners in choosing balanced operating points; and
- stochastic wind modeling is essential for realistically assessing UAV behavior under environmental disturbances.

This study is limited by its use of a 2D kinematic flight model, a fixed swarm size, and the application of NSGA-II only to the representative OU + 150 g scenario due to computational considerations. Future research will address these limitations by:

- Extending the simulation to full 3D flight dynamics, incorporating altitude control and vertical wind components;
- Modeling intra-swarm energy-sharing and cooperative power management;
- Exploring hybrid evolutionary–reinforcement learning frameworks for adaptive multi-agent coordination;
- Incorporating advanced multi-objective optimizers such as NSGA-III, MOEA/D, or SPEA2 for higher-dimensional trade spaces; and
- Developing real-time adaptive optimization pipelines using live flight telemetry for deployment in real-world UAV operations.

Scientific Ethics Declaration

* The author declares that the scientific ethical and legal responsibility of this article published in EPSTEM journal belongs to the author.

Conflict of Interest

* The author declares that he has no conflicts of interest

Funding

* Not applicable

Acknowledgements or Notes

* This article was presented as a poster presentation at the International Conference on Technology, Engineering and Science (www.icontes.net) held in Antalya/Türkiye on November 12-15, 2025.

References

Abeywickrama, H. V., Jayawickrama, B. A., He, Y., & Dutkiewicz, E. (2018). Comprehensive energy consumption model for unmanned aerial vehicles, based on empirical studies of battery performance. *IEEE Access, 6*, 58383-58394.

Alqudsi, Y., & Makaraci, M. (2025). UAV swarms: Research, challenges, and future directions. *Journal of Engineering and Applied Science, 72*, 12.

Arranz, R., Carramiñana, D., de Miguel, G., Besada, J. A., & Bernardos, A. M. (2023). Application of deep reinforcement learning to UAV swarming for ground surveillance. *Sensors, 23*(21), 8766.

Baidya, B., Mondal, A., Mallick, S., & Anamalamudi, S. (2024). Energy-efficient UAV path planning using PSO-ABC algorithm in obstacle-rich environments. *2024 OITS International Conference on Information Technology (OCIT)*, 199–204.

Beni, G. (1988). The concept of cellular robotic system. *Proceedings 1988 IEEE International Symposium on Intelligent Control*, 57–62.

Beni, G., & Wang, J. (1993). Swarm intelligence in cellular robotic systems. In P. Dario, G. Sandini, & P. Aebischer (Eds.), *Robots and biological systems: Towards a new bionics?* (pp. 703–712). Springer.

Cabuk, U. C., Tosun, M., Dagdeviren, O., & Ozturk, Y. (2024). Modeling energy consumption of small drones for swarm missions. *IEEE Transactions on Intelligent Transportation Systems, 25*(8), 10176-10189.

Chen, Y., Chen, R., Huang, Y., Xiong, Z., & Li, J. (2024). Distributed task allocation for multiple UAVs based on swarm benefit optimization. *Drones, 8*(12), 766.

Cosar, M. (2023a). Artificial intelligence technologies and applications used in unmanned aerial vehicle systems. *The Eurasia Proceedings of Science, Technology, Engineering & Mathematics, 26*, 1-12.

Cosar, M. (2023b). Path planning via swarm intelligence algorithms in unmanned aerial vehicle population. *The Eurasia Proceedings of Science, Technology, Engineering & Mathematics, 26*, 439-450.

Di Franco, C., & Buttazzo, G. (2016). Coverage path planning for UAVs photogrammetry with energy and resolution constraints. *Journal of Intelligent & Robotic Systems, 83*(3-4), 445–462.

Duan, P., Yu, Z., Gao, K., Meng, L., Han, Y., & Ye, F. (2024). Solving the multi-objective path planning problem for mobile robot using an improved NSGA-II algorithm. *Swarm and Evolutionary Computation, 87*, 101576.

Galati, G., Primatesta, S., & Rizzo, A. (2023). Auction-based task allocation and motion planning for multi-robot systems with human supervision. *Journal of Intelligent & Robotic Systems, 109*, 24.

Gamil, A., Sheltami, T., Mahmoud, A., & Yasar, A. (2023). Energy-efficient UAVs coverage path planning approach. *Computer Modeling in Engineering & Sciences, 136*(3), 3239-3263.

Gong, H., Huang, B., Jia, B., & Dai, H. (2022). Modelling power consumptions for multi-rotor UAVs. *arXiv*.

Guo, S., Alkouz, B., Shahzaad, B., Lakhdari, A., & Bouguettaya, A. (2023). Drone formation for efficient swarm energy consumption. *arXiv*.

Güven, İ., & Yanmaz, E. (2024). Multi-objective path planning for multi-UAV connectivity and area coverage. *Ad Hoc Networks, 160*, 103520.

Hohmann, N., Bujny, M., Adamy, J., & Olhofer, M. (2021). Hybrid evolutionary approach to multi-objective path planning for UAVs. *2021 IEEE Symposium Series on Computational Intelligence (SSCI)*, 1-8.

Jacewicz, M., Żugaj, M., Głębocki, R., & Bibik, P. (2022). Quadrotor model for energy consumption analysis. *Energies, 15*(19), 7136.

Jiang, H., Lin, S., Chen, J., & Miao, X. (2025). Fusion of cluster analysis and differential particle swarm optimisation for multi-UAV task assignment on power transmission line. *Engineering Computations, 42*(4), 1447–1470.

Lei, Y., & Cheng, M. (2020). Aerodynamic performance of a hex-rotor unmanned aerial vehicle with different rotor spacing. *Measurement and Control, 53*(3-4), 711-718.

Lin, L., Wang, Z., Tian, L., Wu, J., & Wu, W. (2024). A PSO-based energy-efficient data collection optimization algorithm for UAV mission planning. *PLOS ONE, 19*(1), e0297066.

Lones, M. A. (2014). Metaheuristics in nature-inspired algorithms. *Proceedings of the 2014 Annual Conference on Genetic and Evolutionary Computation Companion*, 1419–1422.

Michel, N., Borer, N., Hu, Q., & Kroo, I. (2022). Modeling and validation of electric multirotor unmanned aerial vehicle system energy dynamics. *eTransportation, 12*, 100173.

Morbidi, F., Mariottini, G. L., & Prattichizzo, D. (2016). Minimum-energy path generation for a quadrotor UAV. *IEEE Transactions on Robotics, 32*(3), 785-796.

Na, Y., Li, Y., Chen, D., Yao, Y., Li, T., Liu, H., & Wang, K. (2023). Optimal energy consumption path planning for unmanned aerial vehicles based on improved particle swarm optimization. *Sustainability, 15*(16), 12101.

Opazo, T. I., Raja Zahirudin, R. A., Palacios, J., Schmitz, S., & Langelaan, J. W. (2023). Analytical and experimental power minimization for fixed-pitch coaxial rotors in hover. *Journal of Aircraft, 60*(2), 546–559.

Rosas-Carrillo, A. S., Solís-Santomé, A., Silva-Sánchez, C., & Camacho-Nieto, O. (2025). UAV path planning using an adaptive strategy for the particle swarm optimization algorithm. *Drones, 9*(3), 170.

Tang, G., Xiao, T., Du, P., Zhang, P., Liu, K., & Tan, L. (2024). Improved PSO-based two-phase logistics UAV path planning under dynamic demand and wind conditions. *Drones, 8*(8), 356.

Wang, G., Wang, F., Wang, J., Li, M., Gai, L., & Xu, D. (2024). Collaborative target assignment problem for large-scale UAV swarm based on two-stage greedy auction algorithm. *Aerospace Science and Technology, 149*, 109146.

Xue, T., Zhang, L., Cao, Y., Zhao, Y., Ai, J., & Dong, Y. (2024). Valley path planning on 3D terrains using NSGA-II algorithm. *Aerospace, 11*(11), 923.

Zhang, Z. (2024). Multi-objective optimization method for building energy-efficient design based on multi-agent-assisted NSGA-II. *Energy Informatics, 7*, 90.

Author(s) Information

Mustafa Cosar
Department of Computer Engineering, Hitit University
19030, Corum/Türkiye
Contact e-mail: *mustafacosar@gmail.com*

To cite this article:

Cosar, M. (2025). Swarm intelligence-based energy optimization for UAV mission efficiency. *The Eurasia Proceedings of Science, Technology, Engineering and Mathematics (EPSTEM), 38,* 244-256.